Journal of Sound and Vibration 329 (2010) 994–1006

Contents lists available at ScienceDirect

Journal of Sound and Vibration

journal homepage: www.elsevier.com/locate/jsvi

Wave propagation in a two-dimensional plane straight duct with panels embedded in its sidewalls

A.K. Abramian

Institute of Problems of Mechanical Engineering, Russian Academy of Sciences, Delft University of Technology, The Netherlands

ARTICLE INFO

Article history:
Received 12 December 2008
Received in revised form
26 October 2009
Accepted 26 October 2009
Handling Editor: M.P. Cartmell

ABSTRACT

This paper presents analytical solutions of the problem of two-dimensional pressure wave propagation in a plane straight duct with rigid spring-supported wall panels. The problems of non-stationary and single-frequency pressure wave propagation in a semi-infinite duct with a moving piston and with panels locally embedded in the sidewalls are studied. Rigid panels are embedded in the sidewalls such that they can carry out small amplitude oscillations perpendicular to the main duct axis. The system of the duct with panels acts as a filter. Based on this filter property, which can be described by the panel parameters, a method of computing the acoustic pressure wave distribution in the duct is presented. A wave localisation effect in the duct caused by trapped modes has been found for particular parameters of the sidewall panels.

1. Introduction

Problems of acoustic pressure wave propagation in a duct arise in the design of engineering construction. One of the main issues is the reduction of sound transmission, which can be obtained by the use of acoustic filters composed of special spring-supported panels. The panels radiate pressure waves into the duct that interact with the incoming plane waves. An analytical solution of the aforementioned problem is presented to find the pressure dependence as a function of the coordinate along the duct.

Scientists have been working on related problems for about 40 years, and some interesting results have been achieved. Doak [1] described the practical applications, theoretical background and the principal features of the theory of acoustic fields caused by source distributions in ducts of finite length. According to [1], the pressure perturbation induced by a number of vibrating pistons flush-mounted in the duct walls was found for the case when all pistons vibrate at the same frequency. Huang [2] showed that in the duct, a substantial amount of sound energy can be transferred to the flexural waves on a finite wall panel embedded on the lower duct wall. In the manuscript by Bi et al. [3], the study of sound propagation in a hard-walled circular cylindrical duct lined with non-uniform impedance in the absence of flow has been performed. The liner was piecewise constant along the duct and was allowed to vary arbitrarily along the circumference. In the manuscript by Berengier and Roure [4], with the help of modal theory, precise expressions have been obtained for the acoustic field and the acoustic pressure generated by a real source mounted on a hard-walled waveguide. In the paper by Lapin [5], the solution of the pressure reduction problem of an acoustic wave propagating along a waveguide with a finite panel embedded in one of its sidewalls was obtained. The paper by Vovk and Grinchenko [6] presents studies of the wave propagation problem in a special plane waveguide filled with a liquid. Some parts of this waveguide are hinged elastic plates. A sound energy transfer coefficient has been found numerically [5,6]. The sound field generated by a fluid-loaded structural wave travelling along the boundary of a two-dimensional duct with walls that have smoothly varying properties

E-mail address: andabr33@yahoo.co.uk

0022-460X/$ - see front matter © 2009 Elsevier Ltd. All rights reserved.
doi:10.1016/j.jsv.2009.10.034

has been found in the manuscript by Grant and Lawrie [7]. In the paper by Abramian et al. [8], the problem of localised trapped modes in an infinite-length plane waveguide has been solved. The waveguide has a mass die oscillating in its wall. The frequencies and parameters of the waveguide and the die have been determined for the case when standing waves were initiated in the region of the die and decayed exponentially while moving off this region.

When a sound wave is transmitted along the interior of a duct, the fluid motion is predominantly parallel to the main duct axis, and the wave motion is almost two-dimensional. For a duct having walls with rigid rectangular cross-sections, a propagating wave may be assumed to be two-dimensional if the following condition is met: $b < \pi c/\omega$, where b is the greatest duct width and ω is the oscillation frequency exiting the duct (as shown in the book by Morse [9]). In the present paper, the analytical solution of the problem of two-dimensional pressure wave propagation in a plane straight duct with symmetric rigid spring-supported panels embedded in the sidewalls has been found based on the non-stationary solution obtained for embedded panels.

As an example, the important problem of single-frequency pressure wave propagation in a semi-infinite duct with sidewall panels oscillating in the direction perpendicular to the duct axis has been studied. Doak [1] obtained the solution for the case when sidewall panels performed the prescribed harmonic motion with constant amplitude. In the present paper, the panel motion is a result of the fluid–structure interaction when the piston in the inlet of the duct generates the travelling wave. Huang [2] solved the problem of the wave propagation in the duct with one panel embedded on the lower wall, without considering the distance from the piston that generates the incident wave. The exact solution shown in the present paper enables the analysis of the influence of that factor on the power transmission coefficient for the case of two symmetric sidewall panels. A method is presented to find the panel parameters for which pressure wave reduction occurs. The rest of the paper is divided into five sections:

Section 2. Formulation and setup of the problem. This section presents assumptions and general equations describing the problem.

Section 3. The general case of non-stationary displacement of the panels under the action of radiation pressure is considered. The non-stationary solutions for particular initial conditions are obtained for the case when mass–spring parameters of the panels are the same.

Section 4. For the case of steady-state motion, expressions for the wave pressure and the power transmission coefficient have been obtained. An analysis of the wave pressure reduction due to the panels is given.

Section 5. To investigate the influence of the panel length, rigidity (natural frequency) and a distance from the panel to a duct inlet, the power transmission coefficient dependences of the piston oscillation frequency for various duct parameters have been drawn.

Section 6. Conclusions. Some recommendations on choosing the panel parameters for obtaining a required wave pressure reduction are made.

2. Formulation and setup of the problem

A plane straight semi-infinite anechoic duct of height H filled with an ideal compressible fluid of density ρ_0 is considered. A piston at the duct inlet produces oscillations, which generate a plane (two-dimensional) longitudinal wave in the duct. A section of the rigid walls of the duct between l and L has been replaced by embedded panels (Fig. 1). The panels are rigid bodies on springs. It is assumed that these panels can only oscillate vertically, that is, uniformly in the y-direction. The equations of motion for such panels are differential equations for forced oscillations, where the driving force is the acoustic radiation pressure.

In Cartesian coordinates, the origin of which coincides with the duct inlet, and the x-axis is directed along the lower wall, the equations describing the given problem are

$$\partial^2\phi/\partial x^2+\partial^2\phi/\partial y^2-c^{-2}\partial^2\phi/\partial t^2=0, 0<x<\infty, 0<y<H$$

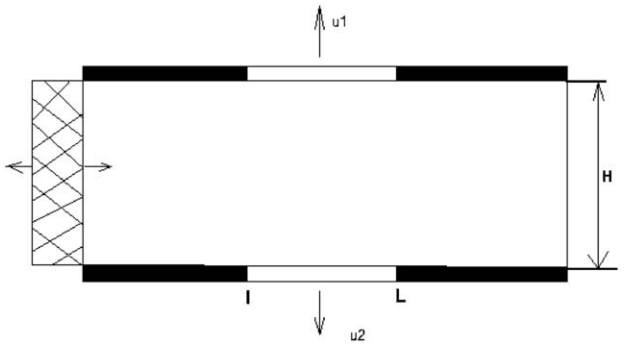

Fig. 1. Duct with embedded panels.

$$M_1\ddot{u}_{1y}+G_1u_{1y}=-\frac{1}{L-l}\int_l^L P(x,y)\,\mathrm{d}x,\ l<x<L,y=0$$

$$M_2\ddot{u}_{2y}+G_2u_{2y}=\frac{1}{L-l}\int_l^L P(x,y)\,\mathrm{d}x,\ l<x<L,y=H$$

$$P=-\rho_0\frac{\partial\varphi}{\partial t} \tag{1}$$

where P is the acoustic pressure, u_{1y}, u_{2y} are panel surface displacement projections along the y-axis, c the acoustic particle velocity, M_1 and M_2 are masses of the panels, G_1 and G_2 are rigidities defining the elastic properties of the panel springs, ϕ the acoustic potential, and ρ_0 the fluid density.

The potential ϕ must satisfy the following boundary conditions.

The fluid particle velocity in the duct inlet is equal to the velocity of the piston when $x=0$:

$\partial\phi/\partial x|_{x=0}=\partial\Delta/\partial t$ ($\partial\Delta/\partial t$ is the speed of piston movement).

At the hard duct walls, the normal component of particle velocity must vanish. At the duct surfaces where panels are embedded, the normal component of particle velocity is equal to the velocity of the panel. As x tends to infinity, a radiation condition applies: that is, as $x\to\infty$, the acoustic disturbances must appear to be coming from the source point, not travelling towards it.

$$\partial\phi/\partial y|_{y=0}=\begin{cases}0, & 0<x<l\\ \partial u_{1y}/\partial t, & l<x<L\\ 0, & x>L\end{cases}$$

$$\partial\phi/\partial y|_{y=H}=\begin{cases}0, & 0<x<l\\ -\partial u_{2y}/\partial t, & l<x<L\\ 0, & x>L\end{cases}$$

$$\phi|_{x\to\infty}\to 0 \tag{2}$$

The effect of fluid loading on the external side of the panel serves to complicate the calculations and is excluded. The last assumption may need further justification. It is necessary to note that when external fluid is not confined, it exhibits evanescent waves with an effect of added mass. Therefore, it is not expected to impact the qualitative results sought in this study. In real applications, however, the external fluid may be confined by a solid wall to form a cavity to prevent noise breakout. The fluid loading inside the cavity is expected to play a similar role as that of the internal loading, and, for the special case of a cavity having a depth equal to the main duct height, the total loading on the panel is simply double that of the present model without external fluid. If the depth is different, the calculations will become rather involved. Therefore, the present study is based on an idealistic model of no external fluid. Thus, it is the field within the duct that is of interest, and the exterior region is assumed to be *in vacuo*.

We have assumed that the panels vibrate with a sufficiently small amplitude that their surfaces practically do not transcend the $y=0$ and H boundaries. At such amplitudes, a phenomenon of possible diffraction caused by the panel edges can be neglected in the solution of the problem. However, the vibrating panels generate a significant radiation pressure in the duct, which must be taken into account. The boundary discontinuity in the panel locations does not result in additional pressure that might be caused by the angle between the panel surface and $y=0$ ($y=H$) duct boundaries (for details, see the book by Mittra and Lee [10]).

3. Non-stationary wave propagation

3.1. General solution of the problem

The general case of non-stationary displacement of the panels under the action of radiation pressure is considered. Using cos-Fourier transform along the x-axis and the Laplace transform with respect to the time variable in the first equation of the system (1) and with the relevant boundary conditions in Eq. (2), and considering trivial initial conditions for t=0, we have

$$\hat{\phi}^F_{yy}-\hat{\phi}^F[(p/c)^2+\lambda^2]=-p\hat{\Delta},0<x<\infty;\ \ 0<y<H$$

$$\hat{\phi}^F_y|_{y=0}=p\hat{u}^F_{1y}(\sin\lambda L-\sin\lambda l)/\lambda,\hat{\phi}^F_y|_{y=H}=-p\hat{u}^F_{2y}(\sin\lambda L-\sin\lambda l)/\lambda \tag{3}$$

where

$$\hat{\phi} = \int_0^\infty \phi(x,y,t)\mathrm{e}^{-pt}\,\mathrm{d}t, \hat{\phi}^F = \left(\frac{2}{\pi}\right)^{0.5} \int_0^\infty \hat{\phi}(x,y,t)\cos\lambda x\,\mathrm{d}x$$

p and λ are Laplace and Fourier parameters, respectively.

The same designations are used for $\hat{\Delta}, \hat{u}_{1y}^F, \hat{u}_{2y}^F$.

The general solution of Eq. (3) has the form:

$$\hat{\phi}^F = A\cosh\gamma y + B\sinh\gamma y + p\hat{\Delta}/\gamma^2$$

$$\gamma^2 = p^2/c^2 + \lambda^2 \tag{4}$$

A and B are determined by the boundary conditions in Eq. (2). Accordingly, the following expressions for the acoustic potential and the acoustic pressure are obtained (with the help of the last equation from Eq. (1)):

$$\hat{\phi}^F(p,\lambda,y) = -p\hat{u}_{1y}^F\frac{\cosh\gamma H}{\gamma\sinh\gamma H}\cosh\gamma y + p\gamma^{-1}\hat{u}_{1y}^F\sinh\gamma y + p\hat{\Delta}/\gamma^2 - \frac{p\hat{u}_{2y}^F\cosh\gamma y}{\gamma\sinh\gamma H}$$

$$\hat{P}^F(p,\lambda,y) = -p^2\rho_0\left[\frac{\hat{\Delta}}{\gamma^2} - \hat{u}_{1y}^F\frac{\cosh\gamma(y-H)}{\gamma\sinh\gamma H} - \hat{u}_{2y}^F\frac{\cosh\gamma y}{\gamma\sinh\gamma H}\right] \tag{5}$$

Performing an inverse cos-Fourier transform and summing up the residues in the complex plane yields:

$$\hat{P}(x,y,p) = -\rho_0 p^2\left\{\hat{\Delta}\frac{c}{p}\mathrm{e}^{-px/c} + 0.5\int_0^\infty \hat{u}_{1y}(p,\zeta)[\hat{\Phi}_1(|x-\zeta|) + \hat{\Phi}_1(|x+\zeta|)]\,\mathrm{d}\zeta + 0.5\int_0^\infty \hat{u}_{2y}(p,\zeta)[\hat{\Phi}_2(|x-\zeta|) + \hat{\Phi}_2(|x+\zeta|)]\,\mathrm{d}\zeta\right\} \tag{6}$$

where

$$\hat{\Phi}_1 = \sqrt{\frac{2}{\pi}}\int_0^\infty \frac{\cosh\gamma(y-H)}{\gamma\sinh\gamma H}\cos\lambda x\,\mathrm{d}\lambda \quad \hat{\Phi}_2 = \sqrt{\frac{2}{\pi}}\int_0^\infty \frac{\cosh\gamma y}{\gamma\sinh\gamma H}\cos\lambda x\,\mathrm{d}\lambda \tag{7}$$

If $x>0$, all poles of the integrands in Eq. (7) lie in the upper half-plane, thus making λ_m equal to

$$\lambda_m = \pm\mathrm{i}\sqrt{p^2/c^2 + \pi^2 m^2/H^2}, m = 0,1,2,\ldots$$

By summing up the residues, one obtains for $\hat{\Phi}_1$ and $\hat{\Phi}_2$ (for mathematical details, see Abrahams [11]):

$$\hat{\Phi}_1 = \frac{1}{H}\left\{-cp^{-1}\mathrm{e}^{-px/c} + \sum_{m=1}^{\infty}(-1)^m\frac{\exp(-\sqrt{\left(\frac{p}{c}\right)^2 + \left(\frac{\pi m}{H}\right)^2}x}{\sqrt{\left(\frac{p}{c}\right)^2 + \left(\frac{\pi m}{H}\right)^2}}\cos\pi m(y-H)/H\right\}$$

$$\hat{\Phi}_2 = \frac{1}{H}\left\{-cp^{-1}\mathrm{e}^{-px/c} + \sum_{m=1}^{\infty}(-1)^m\frac{\exp(-\sqrt{\left(\frac{p}{c}\right)^2 + \left(\frac{\pi m}{H}\right)^2}x}{\sqrt{\left(\frac{p}{c}\right)^2 + \left(\frac{\pi m}{H}\right)^2}}\cos\pi m y/H\right\} \tag{8}$$

To compute the convolution integral in the expression for the pressure, the behaviour of the panel boundary speed function in relation to x should be known. If this relationship is known, one can find the average pressure on the panels. To do this, we have to perform the inverse Laplace transform.

To express the oscillations of the panels as a function of the coordinates, the given boundary conditions (velocities) of the panels in the region $l<x<L$ are considered. Subsequently, the convolution integral for the pressure, Eq. (6), is evaluated for the following three regions:

$0<x<l$, $l<x<L$ and $L<x<+\infty$, with the help of Eq. (8) according to the technique taken from Abramian et al. [8].

The pressure in the aforementioned regions has the following forms:

For $0<x<l$:

$$\hat{P}(x,p,y) = -\rho_0\left\{-cp\hat{\Delta}\mathrm{e}^{-px/c} - \frac{\hat{u}_{1y}+\hat{u}_{2y}}{H}[c^2(\mathrm{e}^{-pL/c} - \mathrm{e}^{-pl/c})\cosh px/c + 2p^2\sum_{m=1}^{\infty}A_m(y,p)\gamma_m^{-1}(\mathrm{e}^{-\gamma_m L} - \mathrm{e}^{-\gamma_m l})\cosh\gamma_m x]\right\} \tag{9}$$

For $l<x<L$:

$$\hat{P}(x,p,y)=-\rho_0\left\{-cp\hat{\Delta}\,e^{-px/c}+\frac{\hat{u}_{1y}+\hat{u}_{2y}}{H}[c^2e^{-px/c}(\sinh px/c-\sinh pl/c)+c^2(e^{-px/c}-e^{-pL/c})\cosh px/c+\sum_{m=1}^{\infty}A_m(y,p)p^2\gamma_m^{-1}(\sinh\gamma_m x-\sinh\gamma_m l)-\sum_{m=1}^{\infty}A_m(y,p)p^2\gamma_m^{-1}\cosh\gamma_m x(e^{-\gamma_m L}-e^{-\gamma_m x})]\right\} \quad (10)$$

For $L<x<+\infty$:

$$\hat{P}(x,p,y)=-\rho_0\left\{-cp\hat{\Delta}\,e^{-px/c}+\frac{\hat{u}_{1y}-\hat{u}_{2y}}{H}[c^2e^{-px/c}(\sinh pL/c-\sinh pl/c)+\sum_{m=1}^{\infty}A_m(y,p)p^2\gamma_m^{-1}e^{-\gamma_m x}(\sinh\gamma_m L-\sinh\gamma_m l)]\right\} \quad (11)$$

where, in Eqs. (9–(11), the following designations are introduced:

$$\gamma_m(p)=\sqrt{p^2/c^2+\pi^2m^2/H^2},A_m(y,p)=(-1)^m\gamma_m^{-1}\left[\cos\frac{\pi m}{H}(y-H)+\cos\frac{\pi m}{H}y\right]$$

The average of the pressure along the panel length has the following form:

$$\frac{1}{L-l}\int_l^L\hat{P}(x,y,p)\,dx,y=0,\quad y=H \quad (12)$$

Then, applying the Laplace transform to the second and the third equations of Eq. (1) and using Eq. (12), we obtain the panel displacement functions $\hat{u}_{2y}$ and $\hat{u}_{1y}$:

$$\hat{u}_{1y}=-\hat{\Delta}\frac{K_1(M_1p^2+G_1)}{(G_1+M_1p^2+K_2)(G_2+M_2p^2-K_2)+K_2^2}$$

$$u_{2y}=\hat{\Delta}\frac{K_1(M_2p^2+G_2)}{(G_1+M_1p^2+K_2)(G_2+M_2p^2-K_2)+K_2^2} \quad (13)$$

where

$$K_1=\frac{c^2\rho_0}{L-l}(e^{-pL/c}-e^{-pl/c})$$

$$K_2=\frac{2\rho_0c^2}{(L-l)H}[(L-l)-cp^{-1}e^{-pL/c}(2\sinh pl/c-\sinh pL/c)+cp^{-1}e^{-pl/c}\sinh pl/c]+\frac{2\rho_0p^2}{(L-l)H}\sum_{m=1}^{\infty}\frac{1}{\gamma_m^2}[(L-l)+\gamma_m^{-1}e^{-\gamma_m L}(2\sinh\gamma_m l-\sinh\gamma_m L)-\gamma_m^{-1}e^{-\gamma_m l}\sinh\gamma_m l]$$

Performing an inverse Laplace transform on Eqs. (9)–(11) in a similar way as the cos-Fourier transform and summing up the residues in the complex plane, one obtains a complete pressure wave distribution in the duct with spring-supported panels.

3.2. Waves caused by the piston kinematic impulse movement

As an example, let us consider the case for the following boundary condition:

$$\left.\frac{\partial\varphi}{\partial x}\right|_{x=0}=\frac{\partial\Delta}{\partial t}=v_0H(t),$$

when the panels' parameters are similar: $G_1=G_2=G$; $M_1=M_2=M$. Here $H(t)$ is the Heaviside function, and v_0 is the piston velocity magnitude. Then $\hat{\Delta}=v_0/p^2$. Substituting this expression into Eq. (11) and applying an inverse Laplace transform with the help of the convolution theorem, one obtains the following expression for the acoustic pressure when $t\geq(x+2L)/c$ and $x>L$:

$$P=\rho_0cv_0\left[H(t-x/c)+\frac{2}{\pi^3\Omega^3\beta^2(1-\varepsilon)}\frac{\rho_0}{\rho}(\sin\omega_1(t-x/c)-0.5\sin\omega_1\left(t-\frac{x+2L}{c}\right)-0.5\sin\omega_1\left(t-\frac{x+l-L}{c}\right)+0.5\sin\omega_1\left(t-\frac{x+l+L}{c}\right)-0.5\sin\omega_1\left(t-\frac{x+2l}{c}\right)+\int_0^t\sin\omega_1(t-\tau)\cdot[\sum_{m=1}^{\infty}[(-1)^m+1]\cdot\int_0^{\tau}(J_0(\pi m\sqrt{\tau_1^2-(x-L)^2/c^2})J_0(\pi m(\tau-\tau_1))+J_0(\pi m\sqrt{\tau_1^2-(x-l)^2/c^2})J_0(\pi m(\tau-\tau_1))\,d\tau_1)\,d\tau))];$$

$$\Omega=\omega_1H/\pi c;\beta=L/H;\varepsilon=l/L;\omega_1=G/M;G_1=G_2=G;M_1=M_2=M;m=1,2,3\ldots \quad (14)$$

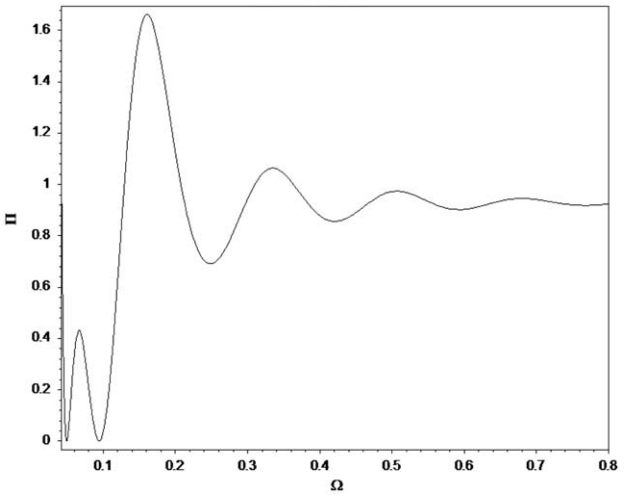

Fig. 2. Relationship between the square of dimensionless pressure in the duct and the panel natural frequency.

In Eq. (14): ω_1 is the panel natural frequency, Ω is the panel non-dimensional natural frequency, ρ is the panel material density, β is an axial distance parameter, ε is the panel size parameter, and $J_0(\pi m(\ldots))$ is the Bessel function of the first kind. From Eq. (14), it follows that at m=1,3,5…$2j$+1 (j=0;1,2,3$\cdots$), the corresponding modes do not contribute to the overall wave packet propagating along the duct. As calculations show, at a large time, only the first term value is significant in the obtained pressure expression. Strictly speaking, though, this presents a large error for those surfaces on which the wave fronts are located. However, if the problem under investigation is considered as an idealisation of some real process in which a wave source generates waves not instantly, then the above-mentioned error is not great. By the analogue of the Saint-Venant principle formulated in the manuscript by Slepian [12], for infinitely long and semi-infinite waveguides, non-stationary waves generated by the panels are local; they attenuate at a duct height distance and are actually wave packets with their width approximately equal to the initial perturbation zone width at the beginning of the process. Subsequently, the wave packet width grows due to dispersion. It has been shown by Slepian [12] that in case of self-balanced and non-self-balanced loads applied simultaneously to the duct inlet, the self-balanced load can be neglected in solving problems of non-stationary wave propagation through ducts filled with fluid for $\Omega < 1$. Thus, as noted by Slepian [12], the Saint-Venant principle is true for problems of non-stationary wave propagation through ducts filled with fluid with some restrictions. However, this conclusion cannot be applied for periodical loads. Rigorous substantiations of the above consideration of the wave packet behaviour for similar problems can be found in the work of Slepian [12].

Fig. 2 presents a diagram of the square of the dimensionless pressure $\Pi = (P/\rho c v_0)^2$ dependences on the panel non-dimensional natural frequency for $\beta = 2$, $\varepsilon = 0.3$, $y = H/5$, $x = 5L$, $\rho_0/\rho = 0.126$ parameters and $t = 14(L/c)$. That time was chosen to satisfy the condition $t \geq (x+2L)/c$ (see Eq. (14)). As seen in Fig. 2, at Ω in the interval $\Omega = 0.042 - 0.128$, the non-dimensional pressure value beyond the panels is $\Pi < 1$. Moreover, there are two values of frequency Ω when $\Pi = 0$. While increasing the parameter ε to 0.8 (short panel), the frequency band where $\Pi < 1$ is shifting to the right along the Ω-axis toward larger frequencies. As calculations show, when time increases to t=100, the number of frequency diapasons at $\Pi < 1$ also increases. However, the width of each of these diapasons decreases. Simultaneously, the right boundary value Ω for the interval where $\Pi < 1$ remains the same. When the parameter β (distance from the duct inlet to the panel) increases, the number of diapasons where $\Pi < 1$ decreases. When the parameter ρ_0/ρ (fluid density/panel material density ratio) increases, the number of diapasons where $\Pi < 1$ increases, as well. Therefore, at a certain selection of panel parameters and location, it is possible to obtain attenuation of the pressure propagating in a particular location along the duct length.

4. Single-frequency approximation

In this section, the steady-state motion is studied in greater detail. Replacing the parameter p in Eqs. (8)–(10) with $+i\omega$, yields the equation for the acoustic pressure in the duct (ω is the angular frequency of the stationary oscillations). In the case of steady-state motion, one obtains the following for the acoustic pressure field:

If $0 < x < l$:

$$P(x,y,t) = \rho_0 e^{-i\omega t}\left\{ i\omega c A_0 e^{i\omega x/c} + \frac{u_{1y} - u_{2y}}{H}[c^2(e^{i\omega L/c} - e^{i\omega l/c})\cos \omega x/c - \omega^2 \sum_{m=1}^{\infty}[(-1)^m + 1]\alpha_m^{-2}(e^{-\alpha_m L} - e^{-\alpha_m l})\cosh \alpha_m x \cos \pi m y/H]\right\} \quad (15)$$

If $l<x<L$:

$$P(x,y,t)=\rho_0 e^{-i\omega t}\left\{i\omega c\Delta_0 e^{i\omega x/c}+\frac{u_{1y}-u_{2y}}{H}[c^2 i e^{i\omega x/c}(\sin\omega x/c-\sin\omega l/c)+c^2(e^{i\omega x/c}-e^{i\omega L/c})\cos\omega x/c - \sum_{m=1}^{\infty}[(-1)^m+1]\omega^2\alpha_m^{-2}\cos\pi m y/H[e^{-\alpha_m x}(\sinh\alpha_m x-\sinh\alpha_m l)-\cosh\alpha_m x(e^{-\alpha_m L}-e^{-\alpha_m x})]]\right\} \quad (16)$$

If $L<x<+\infty$:

$$P(x,y,t)=-\rho_0 e^{-i\omega t}\left\{i\omega c\Delta_0 e^{i\omega x/c}+\frac{u_{1y}-u_{2y}}{H}[c^2 i e^{i\omega x/c}(\sin\omega L/c-\sin\omega l/c) - \sum_{m=1}^{\infty}[(-1)^m+1]\omega^2\alpha_m^{-2}e^{-\alpha_m x}(\sinh\alpha_m L-\sinh\alpha_m l)\cos\pi m y/H]\right\} \quad (17)$$

where $\alpha_m=\sqrt{\pi^2 m^2/H^2-\omega^2/c^2}$ is the exponential coefficient and Δ_0, u_{1y}, u_{2y} are the piston and panel amplitudes, respectively.

The acoustic pressure field behind the panels $x>L$, as a function of the frequency can be analysed as follows. From Eq. (17), one can observe that the pressure field behind the panels can be expressed by the superposition of a radiated two-dimensional single-frequency wave and of waves generated by the oscillations of the panels. Depending on the value of the frequency, an infinite set of two-dimensional acoustic waves represented by the sum in Eq. (17) contains different numbers of waves with decaying amplitudes and periodic waves that propagate along the duct length. By increasing the frequency, propagating waves occur in pairs in the same way as in a duct without panels.

Next, we discuss the range of frequencies limited by the first natural frequency of the duct. As the calculation shows, one may neglect the exponentially decaying modes in the expression for the pressure field for $x>L$ because their pressure can be neglected in comparison with the pressure of the propagating waves at the distance $x>1.5\,L$ behind the panels. The diagram in Fig. 3 presents the dependence of the maximum error (Er) of the coordinate selected for finding the pressure value when the exponentially damped terms in Eq. (17) at the distance $x>1.5\,L$ are neglected (the maximum is reached at $\omega=0.9\pi c/H;\ L/H=1;\ l/L=0.8$).

The value of the error is the ratio of the contribution of the exponentially decaying modes in the pressure to the contribution of the propagating waves. Thus, the pressure field behind the panels has the form:

$$P(x,y,t)|_{x>L}=\rho_0\exp[i\omega(x-ct)/c]\cdot[i\omega c\Delta_0-ic^2(u_{1y}-u_{2y})H^{-1}(\sin\omega L/c-\sin\omega l/c)]=\rho_0 i\omega c\Delta_0\exp[i\omega(x-ct)/c]E(i\omega) \quad (18)$$

where $E(i\omega)=1-2c(u_{1y}-u_{2y})\Delta_0^{-1}\omega^{-1}H^{-1}(\sin\omega L/c-\sin\omega l/c)$ is the complex transfer function of the system.

An expression for the panels displacement functions $u_{2y}(i\omega)$ and $u_{1y}(i\omega)$, involved in the transfer function $E(i\omega)$ for the single-frequency approximation, can be found from the Eq. (13) by replacing the parameter p by $+i\omega$:

$$u_{1y}=-\Delta_0\frac{K_1(i\omega)(G_1-M_1\omega^2)}{(G_1-M_1\omega^2+K_2(i\omega))(G_2-M_2\omega^2-K_2(i\omega))+K_2^2(i\omega)}$$

$$u_{2y}=\Delta_0\frac{K_1(i\omega)(G_2-M_2\omega^2)}{(G_1-M_1\omega^2+K_2(i\omega))(G_2-M_2\omega^2-K_2(i\omega))+K_2^2(i\omega)} \quad (19)$$

where

$$K_1=\frac{c^2\rho_0}{L-l}(e^{i\omega L/c}-e^{i\omega l/c})$$

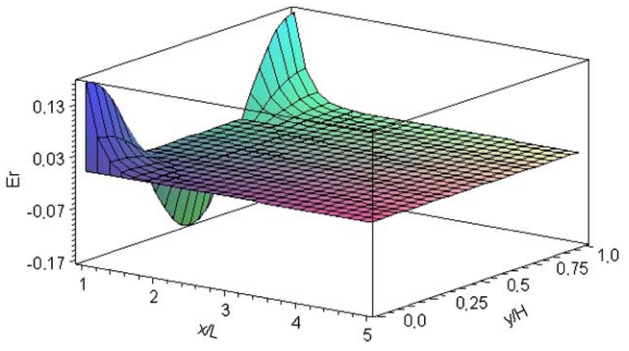

Fig. 3. Relationship between the error and the coordinate.

$$K_2 = \frac{2\rho_0 c^2}{(L-l)H}[(L-l)+\mathrm{i}c\omega^{-1}\mathrm{e}^{\mathrm{i}\omega L/c}(2\sin\omega l/c-\sin\omega L/c)-\mathrm{i}c\omega^{-1}\mathrm{e}^{\mathrm{i}\omega l/c}\sin\omega l/c]$$
$$-\frac{2\rho_0\omega^2}{(L-l)H}\sum_{m=1}^{\infty}\frac{1}{\alpha_m^2}[(L-l)+\alpha_m^{-1}\mathrm{e}^{-\alpha_m L}(2\sinh\alpha_m l-\sinh\alpha_m L)-\alpha_m^{-1}\mathrm{e}^{-\alpha_m l}\sinh\alpha_m l] \quad (20)$$

The expressions for u_{1y}, u_{2y} and for their sum can be analysed as follows.

Assume that the piston frequency satisfies the equation $-M_1\omega^2+G_1=0$. At this frequency, the natural resonance frequency of the panel, $u_{1y}=0$ and $u_{2y}=K_1\Delta_0/K_2$. For this case, it is clear that one panel remains at rest while the other one vibrates with a finite amplitude. If the frequencies of the piston satisfy the following equation: $-(M_1+M_2)\omega^2+G_2+G_1=0$, then $u_{1y}-u_{2y}=0$, and only the travelling waves will exist in the duct.

For the case when $u_{1y}\neq u_{2y}$ and the panels were made from different materials, the complex transfer function $E(\mathrm{i}\omega)$ of the duct can be found after some manipulations of Eq. (18) with the help of Eqs. (19) and (20) and has the form:

$$E(\mathrm{i}\omega)=1+\frac{2(\overline{\omega}_2^2+d\cdot\overline{\omega}_1^2-(1-d)\cdot\overline{\omega}^2)}{\pi^3\beta^2(1-\varepsilon)^2\overline{\omega}}\left(\frac{\rho_0}{\rho}\right)\frac{(D_1C_1N-C_1^2)}{K^2+N^2}+\mathrm{i}\frac{2(\overline{\omega}_2^2+d\cdot\overline{\omega}_1^2-(1-d)\cdot\overline{\omega}^2)}{\pi^3\beta^2(1-\varepsilon)^2\overline{\omega}}\left(\frac{\rho_0}{\rho}\right)\frac{(NC_1^2+KD_1C_1)}{K^2+N^2} \quad (21)$$

where

$$C_1=2\sin\frac{\pi}{2}\beta\overline{\omega}(1-\varepsilon)\cos\frac{\pi}{2}\beta\overline{\omega}(1+\varepsilon);\ D_1=2\sin\frac{\pi}{2}\beta\overline{\omega}(1-\varepsilon)\sin\frac{\pi}{2}\beta\overline{\omega}(1-\varepsilon)$$

$$\beta=L/H;\ \varepsilon=l/L;\ \overline{\omega}=\omega H/\pi c;\ \overline{\omega}_1=G_1H/\pi cM_1;\ \overline{\omega}_2=G_2H/\pi cM_2;$$

$$K=(\overline{\omega}_2^2-\overline{\omega}^2)(\overline{\omega}_1^2-\overline{\omega}^2)+2\left(\frac{\rho_0}{\rho}\right)\frac{(\overline{\omega}_2^2-d\cdot\overline{\omega}_1^2-(1-d)\cdot\omega^2)}{\pi^2\beta(1-\varepsilon)}A_1$$

$$A_1=1-\overline{\omega}^2\sum_{m=1}^{\infty}\frac{1}{m^2-\overline{\omega}^2}+\frac{\omega^2}{\pi\beta(1-\varepsilon)}\sum_{m=1}^{\infty}\frac{1}{(m^2-\overline{\omega}^2)^{1.5}}+\frac{C_1^2}{\pi\beta(1-\varepsilon)\overline{\omega}};$$

$$\sum_{m=1}^{\infty}\frac{1}{m^2-\overline{\omega}^2}=-\frac{\pi}{2\overline{\omega}}\operatorname{ctg}\pi\overline{\omega}+\frac{1}{2\overline{\omega}^2};\ d=\frac{M_1}{M_2};\ M_1=\rho L(1-\varepsilon)$$

$$N=\left(\frac{\rho_0}{\rho}\right)\frac{(\overline{\omega}_2^2-d\cdot\overline{\omega}_1^2-(1-d)\cdot\omega^2)}{\pi^2\beta(1-\varepsilon)}B_1;\ B_1=\frac{D_1\sin\pi\beta\varepsilon\overline{\omega}-C_1\cos\pi\beta\overline{\omega}}{\pi\beta\overline{\omega}(1-\varepsilon)} \quad (22)$$

$\overline{\omega}$ is the non-dimensional frequency of the piston, $\overline{\omega}_1$, $\overline{\omega}_2$ are the non-dimensional natural frequencies of the panels, and d is the ratio of the panel masses. The case when $d=1$ corresponds to the case when both panels were made from the same material.

Tedious calculations of the value of the complex transfer function $E(\mathrm{i}\omega)$ and the power transmission coefficient of the duct in the case when $u_{1y}\neq u_{2y}$ can be simplified for the panels with the same parameters, $M_1=M_2=M$ and $G_2=G_1=G$. $E(\mathrm{i}\omega)$ for this case can be found by evaluating the function $K_2(\mathrm{i}\omega)$. To obtain an expression for $K_2(\mathrm{i}\omega)$ for practical systems, it suffices to take into consideration the amplitude of the first mode, $m=1$. Then the complex transfer function $E(\mathrm{i}\omega)$ has the following form:

$$E(\mathrm{i}\omega)=1-4\pi^{-3}(\rho_0/\rho)\frac{C_1^2}{\beta^2(1-\varepsilon)^2\overline{\omega}(\overline{\omega}_1^2-\overline{\omega}^2)}+\mathrm{i}4\pi^{-3}(\rho_0/\rho)\frac{C_1D_1}{\beta^2(1-\varepsilon)^2\overline{\omega}(\overline{\omega}_1^2-\overline{\omega}^2)} \quad (23)$$

where

$$C_1=2\sin\frac{\pi}{2}\overline{\omega}\beta(1-\varepsilon)\cos\frac{\pi}{2}\overline{\omega}\beta(1+\varepsilon);\ D_1=2\sin\frac{\pi}{2}\beta\overline{\omega}(1+\varepsilon)\sin\frac{\pi}{2}\overline{\omega}\beta(1-\varepsilon) \quad (24)$$

The effect of the pressure wave propagation on the dynamic behaviour of the panels can be analysed by the amplitude–phase characteristics of the system, that is, the modulus and the phase of the complex transfer function in relation to the radiation frequency. For different frequencies, the transfer function modulus can be either greater or less than unity, corresponding respectively to the increase or the decrease in the pressure at the duct inlet. The maximum of the transfer function modulus follows from: $G-M\omega^2=0$. This is a resonance condition, implying that the radiation frequency coincides with the frequency of the panel and that the system has a resonance with an infinite value of $|E(\mathrm{i}\omega)|$. At resonance, the phase shift between a radiated plane wave and a wave produced by the panels is equal to $\pi/2$, whereas the displacement and velocity of the panels reach maximal values. It is evident that when there is harmonic radiation with frequencies close to natural frequencies of the panels, one can expect a sharp growth of the harmonic amplitudes.

Hence, it follows that the range of frequencies of the acoustic radiation waves that are to be suppressed should be significantly far from the resonance region. This fact must be taken into account in practical applications.

Another interesting phenomenon, that of trapped modes, may occur in the duct. The frequencies for which such a phenomenon occurs are ones corresponding to standing waves in the duct for $x>L$. The presence of such waves in the total

wave packet points to the existence of a mixed natural spectrum of differential operators describing the behaviour of hydroelastic systems (see Abramian et al. [8]). To find such frequencies, one comes to the following system of equations:

$$\begin{cases} 1 - SC_1^2 = 0 \\ SC_1 D_1 = 0 \\ S = 4\pi^{-3}(\rho_0/\rho)/\beta^2(1-\varepsilon)^2\overline{\omega}(\overline{\omega}_1^2 - \overline{\omega}^2) \end{cases} \tag{25}$$

It follows from the second equation of the system that $D_1 = 0$. Then the corresponding frequency becomes $\overline{\omega}_j = 2j/\beta(1+\varepsilon)$, $j = 1, 2, \ldots$ The number of these frequencies can be found from the condition $\overline{\omega}_j < \pi c/H$; then $j < (L+l)/2H$. To satisfy the first equation of Eq. (25), it is necessary that $SC_1^2 = 1$. The natural frequency corresponding to this case panel may be obtained by substituting the value $\overline{\omega}_j$ found from the second equation of Eq. (25) into the first equation.

Additionally, by inserting the following designation of the ratio $\overline{\omega}_1/\overline{\omega}_j = \alpha$, one obtains from the first equation of Eq. (25) the expression for α:

$$\alpha^2 = 1 + \frac{2\beta(1+\varepsilon)^3}{p^3 j^3 (1-\varepsilon)^2}\left(\frac{\rho_0}{\rho}\right)\sin^2\left(pj\frac{1-\varepsilon}{1+\varepsilon}\right) \tag{26}$$

Thus, a trapped-mode frequency may exist only at specific values of β and ε parameters. In other words, when a trapped-mode exists, a panel natural frequency can be found for a fixed panel length and distance from the panel to the duct inlet. The natural frequency of the panel depends on its rigidity and its mass; therefore, to obtain the trapped-mode frequency of a duct, the aforementioned parameters should be selected.

In that case, one can always find values of parameters G and M that satisfy Eq. (25). As a result of the trapped mode phenomenon, only transverse standing waves, which vanish exponentially along the duct length, will occur downstream from the panels. That phenomenon can be explained as follows. All of the fluid mass at the panel moves together with the panel (i.e., the fluid is "adapted" to the panel). Thus, the fluid effect can be considered as an added mass of the panel. Hence, the interaction of the fluid and rigid panels with fixed kinematics and a finite number of degrees of freedom can lead to standing localised mode formation. Conversely, the interaction of the fluid and homogeneous elastic panels with an infinite number of degrees of freedom cannot lead to the standing localised mode formation as was shown by Abramian et al. [8]. For the elastic structures, their surface can be considered as an infinite number of wave sources. In contrast to the case of rigid panels, these sources are non-coherent, and their summarised action cannot produce the well localised waves (elastic structure and the fluid cannot be matched).

5. Results and discussion

To investigate the influence of the panel length, rigidity (natural frequency) and distance from the panel to a duct inlet, the power transmission coefficient dependences on the plunger oscillation frequency for various β and ε parameters have been plotted. The power transmission coefficient is defined as $\Phi = |E(i\overline{\omega})|^2$. From the dependences given in Figs. 4–6, the following conclusions can be derived.

For a short panel ($\varepsilon = 0.8$; $\rho_0/\rho = 0.126$) located far from the duct inlet ($\beta = 10$) and the panel natural frequency $\overline{\omega}_1 = 0.1716$, which enables trapped mode existence, the frequency range when $\Phi < 1$ is as follows: $0.0634 < \overline{\omega} < 0.137$ (Fig. 4). At the frequency $\overline{\omega} = 0.11$, the trapped mode effect $\Phi = 0$ is observed. At $\overline{\omega} > 0.132$, the magnitude $\Phi \geq 1$, and the panel practically does not weaken the propagating wave. At the frequency $\overline{\omega} = 0.1716$, resonance that corresponds to a sharp Φ increase is observed. Increasing the panel length (and therefore its mass), i.e., parameter ε=0.1, the frequency range at the same distance from the duct inlet (β=10) when $\Phi < 1$ is shifted: $0.11 < \overline{\omega} < 0.183$ (Fig. 4). Over the rest of the range up to the first cut-off frequency, one has $\Phi \geq 1$. Thus, it can be concluded that if ε changes 8 times, it has a small influence on the range width where $\Phi < 1$. In the case where the panel rigidity increases such that its natural frequency does not correspond to the trapped-mode frequency but instead remains close to it ($\overline{\omega}_1 = 0.2$), the width of the frequency range when $\Phi < 1$ remains approximately the same (Fig. 4).

The broken line in Fig. 4 shows the minimum corresponding to $\Phi = 0.085$. However, when further increasing the panel rigidity and its natural frequency up to $\overline{\omega}_1 = 0.8$, the behaviour of the dependence $\Phi(\overline{\omega})$ changes. As seen from the dotted curve in Fig. 4, the magnitude $\Phi = 1$ is observed over the whole range of frequencies, excluding a narrow resonance zone. Therefore, only a special selection of the panel parameters (rigidity and mass) may provide the best filtration and $\Phi < 1$ values.

When the distance from the panel to the duct inlet decreases to below that of the aforementioned cases, for example, at β=2, ε=0.8, the frequency range when $\Phi < 1$ becomes broader than for β=10 and ε=0.8′ in particular: $0.36 < \overline{\omega} < 0.59$ (dotted curve in Fig. 5). The natural frequency of the panel $\overline{\omega}_1 = 0.6278$ corresponds to the trapped modes effect. When the length (mass) of the panel is reduced, then the frequency range for $\Phi < 1$ becomes slightly broader. The continuous curve in Fig. 5 shows this effect for β=2, ε=0.2, when the range within which $\Phi < 1$ is as follows: $0.6 < \overline{\omega} < 0.84$. All figures also show the frequency ranges where $\Phi > 1$.

The case when $\Phi < 1$ represents that the pressure wave amplitude in the duct behind the panels is always less than the amplitude of the single-frequency plane waves that propagate in the duct without panels under the same radiation conditions. It follows that there is a range of frequencies of wave radiation for which the transfer function modulus has a

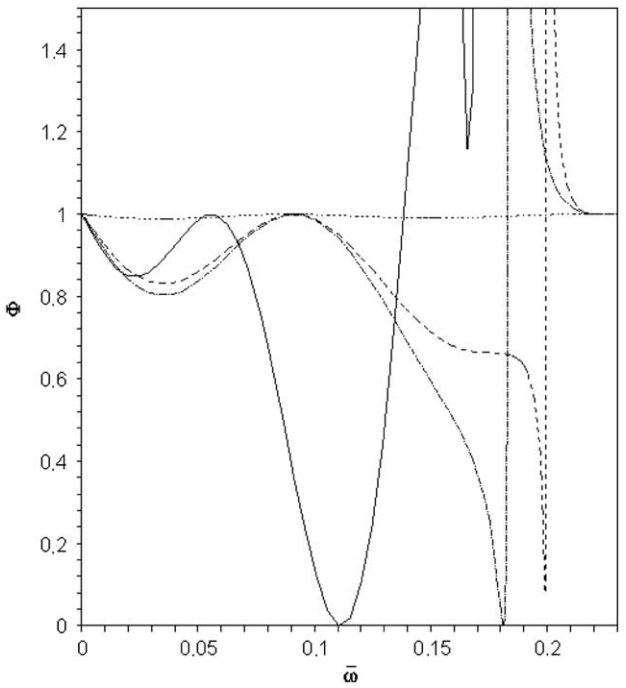

Fig. 4. The power transmission coefficient dependence on the non-dimensional frequency for a steel panel. The continuous line is for $\beta = 10$; $\varepsilon = 0.8$, and the dash–dot line is for $\beta = 10$; $\varepsilon = 0.1$, broken line is for $\beta = 10$; $\varepsilon = 0.1$; $\overline{\omega}_1 = 0.2$, dot line is for $\beta = 10$; $\varepsilon = 0.1$; $\overline{\omega}_1 = 0.8$.

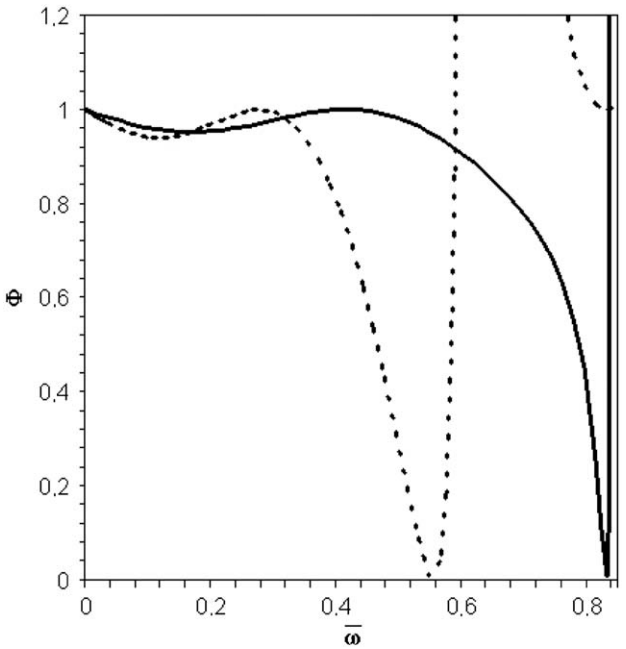

Fig. 5. The power transmission coefficient dependence on the non-dimensional frequency for a steel panel. The dotted line is for $\beta = 2$; $\varepsilon = 0.8$. The continuous line is for $\beta = 2$; $\varepsilon = 0.2$.

minimum value; in other words, there is a frequency range of radiation with optimal filtering. Suppose that the range of the frequencies of the radiated waves to be suppressed and the geometric dimensions of the duct are given. Then by using the expression for Φ, one can find the values of the geometric and dynamic parameters for which the acoustic radiation pressure at the duct inlet reaches the minimal value.

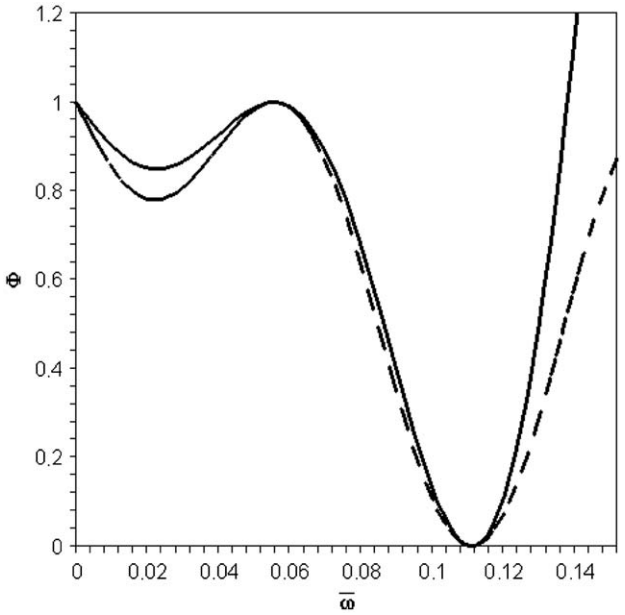

Fig. 6. The power transmission coefficient dependence on the non-dimensional frequency for rubber and steel panels and a duct filled with water. The continuous line is for a steel panel, and the broken line is for a rubber panel ($\beta = 10$; $\varepsilon = 0.2$).

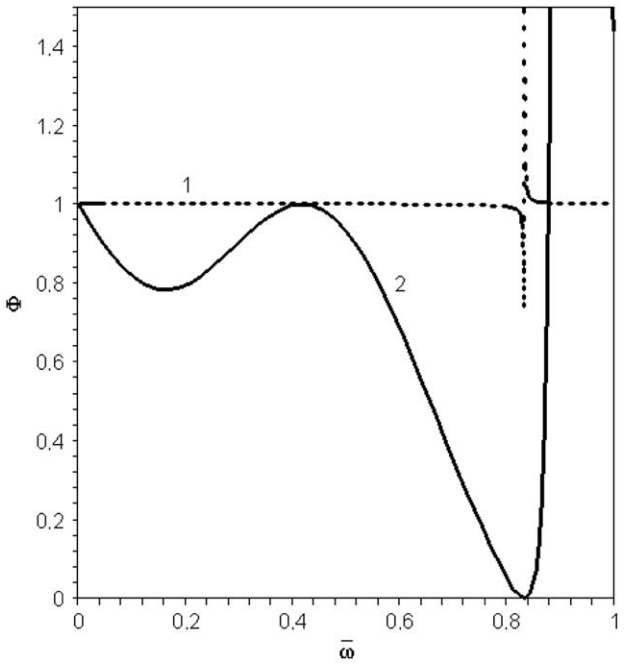

Fig. 7. The power transmission coefficient dependence on the non-dimensional frequency for a short rubber panel. The continuous line is for the duct filled with liquid, and the broken line is for the duct filled with air ($\beta = 2$; $\varepsilon = 0.2$).

The power transmission coefficient can be bigger than 1 for the steady-state motion because two waveguides are connected: one is of the finite length l, and another is of semi-infinite length (for $x > L$). The waves transmitted upstream of the panels in the steady-state motion are the result of a multiple reflection of waves in the following region of the duct length $0 < x < L$. Depending on the phase difference between the incident and reflected waves, the wave packet transmitted downstream can have greater or lesser power than does the incident wave itself. For this reason, for particular values of the duct parameters, the power transmission coefficient can be greater than 1. In that case, the panels cannot be used for filtering.

Diagrams in Figs. 4 and 5 have been constructed for the duct filled with water and for steel panels. Let us investigate the effect of the panel material on the power transmission coefficient Φ. When the panel material is, for example, rubber ($\rho_0/\rho = 0.73$), and $\beta = 10$; $\varepsilon = 0.8$; then $\overline{\omega}_1 = 0.339$.

The diagram in Fig. 6 shows that the frequency range when $\Phi < 1$ increases by $\Delta\overline{\omega} = 0.03$ in comparison with the case when the panel material is steel. It should be mentioned that $\Delta\overline{\omega}$ is a value related to $\pi c/H$; thus, the frequency range where $\Phi < 1$ can reach hundreds of hertz. When rubber panels are used, the frequency range where $\Phi < 1$ for parameters $\beta = 2$; $\varepsilon = 0.2$ increases by $\Delta\overline{\omega} = 0.034$.

When the duct is filled with air and the panel is made of rubber, the parameter $\rho_0/\rho = 0.00088$. Fig. 7 presents the relationship between Φ and $\overline{\omega}$ at $\beta = 2$ and $\varepsilon = 0.2$ for the cases when the duct is filled with air and with liquid. The width

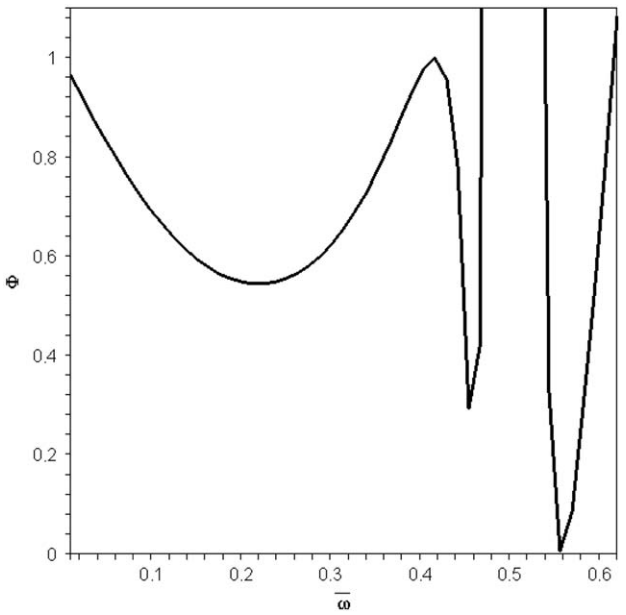

Fig. 8. The power transmission coefficient dependence on the non-dimensional frequency when the panels have different $\overline{\omega}_1$ and $\overline{\omega}_2$ ($\beta = 2$; $\varepsilon = 0.2$; $\overline{\omega}_1 = 0.8$; $\overline{\omega}_2 = 0.5$; $\rho_0/\rho = 0.128$; $d = 2$).

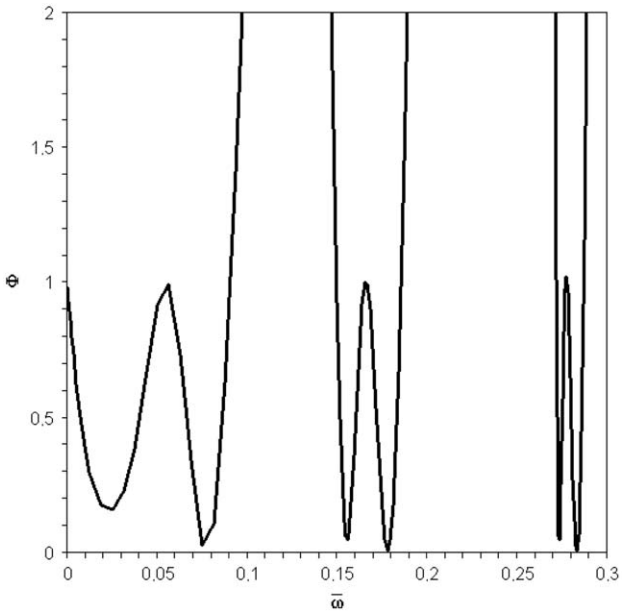

Fig. 9. The power transmission coefficient dependence on the non-dimensional frequency when the panels have different $\overline{\omega}_1$ and $\overline{\omega}_2$ ($\beta = 10$; $\varepsilon = 0.8$; $\rho_0/\rho = 0.73$; $d = 2$).

of the frequency range with $\Phi<1$ is $\Delta\overline{\omega}=0.0034$ for the case when the duct is filled with air. Thus, the absolute range width can equal several Hertz.

Let us study a case when the panels have different $\overline{\omega}_1$ and $\overline{\omega}_2$ (different G_1, G_2, M_1, M_2). Using Eqs. (21) and (22), a diagram of $\Phi(\overline{\omega})$ was constructed at the similar values of β and ε as for the case when $\overline{\omega}_1$ and $\overline{\omega}_2$ are the same and the duct is filled with water. Diagrams of $\Phi(\overline{\omega})$ for parameters $\beta=2$; $\varepsilon=0.2$; $\overline{\omega}_1=0.8$; $\overline{\omega}_2=0.5$; $\rho_0/\rho=0.126$; $d=2$ are given in Fig. 8. From the diagrams, it can be seen that several frequency ranges exist with $\Phi<1$. One such range has $\Delta\overline{\omega}=0.39$, and two others have $\Delta\overline{\omega}=0.05$; $\Delta\overline{\omega}=0.078$. The same type of behaviour of $\Phi(\overline{\omega})$ has been obtained for $\beta=10$, $\varepsilon=0.8$, $\rho_0/\rho=0.73$; $d=2$ (Fig. 9). Analysing these and other diagrams at various panel parameters, one can conclude that the number of ranges with $\Phi<1$ increases when the values of the panel natural frequencies are different. The case when $d=1$ shows the same qualitative results.

6. Conclusions

An analytical approach to determine the pressure wave distribution in a plane straight duct with a local mass–spring behaviour of the sidewalls along which non-stationary and stationary plane waves are propagating has been presented and calculated. In the low frequency regime, the panels reduce wave amplitudes and therefore act as filters. There is a frequency range for which the power transmission coefficient reaches a minimal value. Only specific selection of the panel parameters (rigidity and mass) may provide the best filtration and $\Phi<1$ values. At the same time, for a particular distance from the duct inlet and the length of panels, the power transmission coefficient can be greater than 1. That phenomenon occurs because of multiple reflections of the waves in the region between the duct inlet and the edge of panels ($0<x<L$).

A trapped-modes phenomenon occurs at some values of the frequencies that correspond to standing waves in the duct for $x>L$. These frequencies can be located above or below the first cut-off frequency of the duct. That phenomenon is possible only for particular values of the panels and duct parameters. The effect of acoustic filtering in the duct by sidewall panels is due to the interaction of the waves generated by the piston and those reflected by the panels. Oscillating panels take their energy from the transmitted wave energy, thus providing a reduction mechanism. From the above given investigation, it follows that the use of panels for reducing noise and pressure vibration levels of flows in hydraulic ducts can be very efficient. The exact analytical expressions obtained for the power transmission coefficient may serve as a foundation for engineering methods for the calculation and design of filters in a number of applications such as machine building.

Acknowledgement

The author is grateful to NWO, The Netherlands Organization for Scientific Research, for support and opportunity to work for six months at the University of Technology Delft.

References

[1] P.E. Doak, Excitation, transmission and radiation of sound from source distributions in hard-walled ducts. Finite length (I): the effects of duct cross-section geometry and source distribution space–time pattern, *Journal of Sound and Vibration* 31 (1) (1973) 1–72.
[2] L. Huang, A theoretical study of passive control of duct noise using panels of varying compliance, *Journal of the Acoustical Society of America* 109 (6) (2001) 2805–2814.
[3] W.P. Bi, V. Pagneux, D. Lafarge, Y. Auregan, Modeling of sound propagation in a non-uniform lined duct using a multi-modal propagation method, *Journal of Sound and Vibration* 289 (4–5) (2006) 1091–1111.
[4] M. Berengier, A. Roure, Broad-band active sound absorption in a duct carrying uniformly flowing fluid, *Journal of Sound and Vibration* 68 (3) (1980) 437–449.
[5] A.D. Lapin, Method of low frequency noise isolation in waveguide, *Acoustical Journal* 16 (12) (1970) 281–285.
[6] I.V. Vovk, V.T. Grinchenko, Plunger radiation into plane waveguide with elastic plates, *Acoustical Journal* 22 (5) (1976) 771–774.
[7] A.D. Grant, J.B. Lawrie, Propagation of fluid loaded structural waves along a duct with smoothly varying bending characteristics, *The Quarterly Journal of Mechanics and Applied Mathematics* 53 (2) (2000) 299–321.
[8] A.K. Abramian, D.A. Indeijchev, S.A. Vakulenko, Wave localization in hydroelastic systems, *Flow, Turbulence and Combustion* 61 (1999) 1–20.
[9] P.M. Morse, K.V. Ingard, *Theoretical Acoustics*, Princeton University Press, Princeton, NJ, 1986.
[10] R. Mittra, S.W. Lee, *Analytical Techniques in the Theory of Guided Waves*, Collier-Macmillan, London, 1971.
[11] I.D. Abrahams, Scattering of sound by finite elastic surfaces bounding ducts of cavities near resonance, *The Quarterly Journal of Mechanics and Applied Mathematics* 35 (1) (1982) 91–101.
[12] L.I. Slepian, *Non-Steady-State Elastic Waves*, Sudostroenie, Leningrad, 1972 (in Russian).